Journal of Applied Polymer Science

Synthesis of Porous Al_2O_3-PVDF Composite Separators and Their Application in Lithium-Ion Batteries

Huifeng Wang,[1] Haibin Li,[1] Lijun Yu,[1] Yanmei Jiang,[2] Kaixue Wang[2]

[1]School of Mechanical Engineering, Shanghai Jiao Tong University, Shanghai 200240, China

[2]School of Chemistry and Chemical Engineering, Shanghai Jiao Tong University, Shanghai 200240, China

Correspondence to: H.B. Li (E-mail: haibinli@sjtu.edu.cn)

ABSTRACT: In this article, a modified tape casting method is employed by dispersing and ball milling of Al_2O_3 powders in the poly (vinylidene fluoride) polymer, with the aim of developing uniform nanocomposite separators in the lithium-ion cell system. The surface morphology, pore structure, heat-resisting property, infrared property, and cell performance of the nanocomposite separators are investigated. The experimental results indicate that ball milling plays an important role in yielding homogeneous, porous nanocomposite separator membranes. The developed separator membranes exhibit high thermal stability and excellent electrochemical performance, therefore, are promising for use in the lithium-ion cell systems. © 2013 Wiley Periodicals, Inc. J. Appl. Polym. Sci. 130: 2886–2890, 2013

KEYWORDS: membranes; composites; electrochemistry

Received 12 December 2012; accepted 4 May 2013; Published online 11 June 2013

DOI: 10.1002/app.39499

INTRODUCTION

A separator is essential for the components of a lithium-ion battery (LIB). Currently, most LIBs use conventional microporous polyolefin membranes as the separators. Microporous polyolefin membranes have a lot of advantages,[1–4] however, they still suffer from low thermal stability, low porosity, and poor wettability in polar electrolyte solvents, which seriously limit the energy density and rate capability of rechargeable LIBs.[5–7] Therefore, it is imperative to develop a new separator with a small pore size and volume, high interfacial properties, and stable electrochemical performance for application in the LIB.

An inorganic-based composite separator, or "ceramic-based separator" (CS), is a porous mat made of ultrafine inorganic particles bonded using a small amount of binder. Due to the high hydrophilicity and high surface area of the small inorganic particles with strong affinity toward polar solvents, such separators exhibit exceptional wettability with all non-aqueous liquid electrolytes,[7] based on polar aprotic solvents (typical examples of which are organic ethers, esters and alkyl carbonates). Meanwhile, these separators have extreme thermal stability at high temperatures. Therefore, the inorganic-based composite separators with excellent wettability and zero shrinkage are highly desirable for the development of large-size Li-ion batteries. Much research[8–19] has been performed recently to search for a series of separators combining the characteristics of ceramic materials and microporous polymer membranes or polymeric non-woven. For the inorganic-based composite separators, much previous work was focused on the membranes composed of ceramic material and either poly (vinylidene fluoride) (PVDF)-based polymers or their blends with other polymers. Early reports were given by Prosini et al.[20] who dispersed metal oxides powders (γ-$LiAlO_2$, Al_2O_3, MgO, respectively) into a PVDF–HFP solution. Ding et al.[21] and Kim et al.[22] investigated TiO_2/PVDF and TiO_2/PVDF–HFP composite separators respectively. Wachtler et al.[23] studied PVDF/SiO_2 gel polymer electrolyte separators for a Li-ion battery. The composite P(VDF-HFP)/SBA-15 (silica) polymer electrolyte separators with high discharge capacities were reported by Yang et al.[24] Stephan et al.[25] synthesized P(VDF-HFP) composite polymer electrolyte separators with two different sizes of aluminum oxyhydroxide ($AlO[OH]_n$) for Li-ion batteries. Jeong and Lee[26] reported SiO_2 nanoparticles embedded in a polymer matrix hence the establishment of a highly ordered nanoporous structure. Subramania et al.[27] studied a novel composite micro-porous polymer electrolyte membrane based on optimized composition of PVDF-co-HFP-ZrO_2. Zhang et al.[28] investigated molecular sieves of MCM-41 modified with sulfated zirconia (SO_4^{2-}/ZrO_2) composite polymer films for lithium-ion batteries. The ceramic materials used in these separators are alumina, silica, zirconia, titanium dioxide or their mixture, and their particle size is required to be of nano-size. Since the inorganic particles are easy to form aggregates or agglomerates, sonication and ball milling had to be used to distribute the inorganic particles evenly in the solvents to possibly form a uniform solution.[9]

© 2013 Wiley Periodicals, Inc.

In this article, we extend the study by reporting the characteristics and properties of a LIB having the optimized Al_2O_3-based composite as the separator and $Li_4Ti_5O_{12}$-TiO_2 as the anode material. Small Al_2O_3 nanoparticles were chosen and uniformly dispersed in polymer binder by ball milling to provide the opportunity to obtain homogenous porous membrane separator. The morphology, thermal stability, pore-size distribution, infrared analysis, the charge/discharge property, and cycle performance of the separator were investigated.

EXPERIMENTAL

Materials

The CS membranes were synthesized from ceramic powder and a polymer binder. Nano-sized aluminum oxide powders (Al_2O_3, Xuan Cheng Jing Rui New Material Co.), PVDF (Sigma-Aldrich), and *N*-methyl-2-pyrrolidone (NMP, Sinopharm Chemical Reagent Co.) were used as inorganic particle, polymer, and solvent, respectively. All these reagents were used as received without further purification or modification.

Synthesis of CS Membranes

An appropriate amount of PVDF was dissolved in NMP at 50°C for 1 h to form a viscous polymer solution, then the suitable amounts of Al_2O_3 powders without any surface modification were added into the solution and continuously stirred for 1 h, followed by ball milling in a planetary ball-mill apparatus (QM-3SP2, NanDa Instrument Plant) for 72 h in air at room temperature to form a uniform dispersion and made into slurries. Agate balls and a 100 mL agate vial were used during ball milling and the rotating speed was fixed at 350 rpm. Thereafter, the CS membranes were fabricated from the slurry using a doctor blade and then were dried to evaporate the NMP at 80°C. The composite membranes could be easily detached from the glass plates after drying by mechanical means such as careful scraping or peeling. The total thicknesses of the CS membranes were kept at about 25 μm after drying in order to avoid losing the high energy density, which is one of the most important advantages of lithium-ion batteries.[29]

Several CS membranes of different Al_2O_3 powder contents were prepared. The weight ratios of Al_2O_3 powder and polymer binder of the CS membranes are given in Table I, where P/B ratio indicates the weight ratio of powder to binder.

Characterization

The morphologies of the CS membranes were examined by scanning electron microscope (Sirion 200, FEI). The pore size distributions of the CS membranes were measured by mercury intrusion porosimeter (Autopore IV 9500, Micromertitics). The heat stability of the CS membranes was reflected by shape change before and after heat treatment at designated temperatures. The formation of different phases was confirmed by Fourier transform infrared attenuated total reflection (FTIR-ATR) spectra, obtained by means of FTIR spectrometer (Nicolet 6700; Thermo Electron Corporation). For the measurement of electrochemical performance, a liquid electrolyte of 1 *M* $LiClO_4$ in ethylene carbonate (EC)/diethyl carbonate (DEC) (EC/DEC = 1/1, v/v) was employed. The CR 2016 coin-type cells were assembled by sandwiching the separator between a $Li_4Ti_5O_{12}$-TiO_2 and a metal lithium foil as counter electrode and then activated by filling the liquid electrolyte. Carbon black was used as a conductive agent in the electrode and PVDF was used as a binder of these active materials, conductive agent, and current collector. These cells were assembled in an argon-filled glove box. Charge-discharge and cycle performance measurements of the cells were performed using a battery test system (LAND CT2001A model; Wuhan Jinnuo Electronics Co.). The cells were galvanostatically discharged and charged in the range of 1.0–2.5 V (vs. Li^+/Li) under a constant current density of 0.1 A g^{-1} at room temperature.

Table I. Composition of the CS Membranes

Particle size (nm)	Samples	Al_2O_3:PVDF	P/B ratio
30	A	3 : 2	1.5
30	B	1 : 2	0.5

RESULTS AND DISCUSSION

Temperature-related safety issues are mostly related to the dimensional shrinking or melting of the separator. Therefore, in order to compare the differences in the heat-resistant properties of the CS membranes with different Al_2O_3 contents, the separators were put into an oven and kept at 150°C for 30 min. Photographs of the CS membranes with different Al_2O_3 contents and pure PVDF membrane (sample C) before and after heat treatment are shown in the top and bottom of Figure 1, respectively. As seen in Figure 1, sample C as a semi-crystalline polymer underwent the highest degree of shrinkage during exposure to the high temperature conditions, which may result in physical contact between the anode and the cathode. The lowest degree of shrinkage was obtained with sample A, suggesting

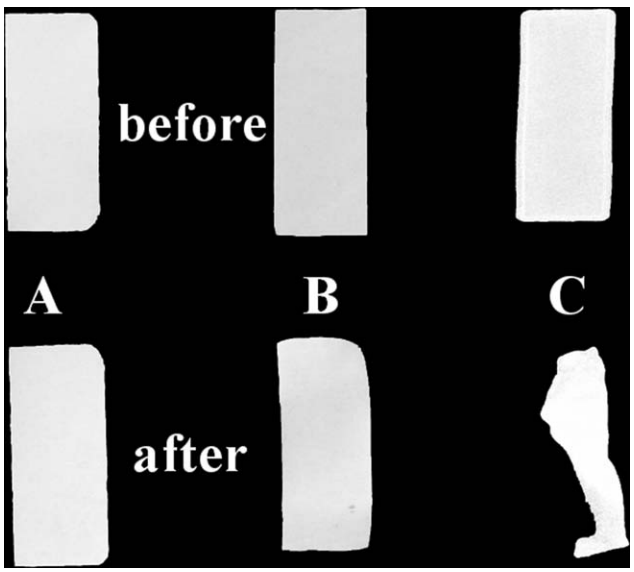

Figure 1. Photographs of CS membranes with different Al_2O_3 contents and pure PVDF membrane before and after being kept at 150°C for 30min. Left to right: sample A, sample B, and sample C.

that thermal stability can indeed be enhanced by adding the heat-resistant Al_2O_3 nanoparticles (coefficient of thermal expansion: α-Al_2O_3 8.5 × 10^{-6}°C^{-1}[30]) into polymer. Moreover, the larger the amount of Al_2O_3 powder, the smaller the shrinkage. The result verifies that the introduction of Al_2O_3 powder is effective in improving the thermal performance of separators.[31]

Figure 2(a) and (b) shows surface SEM images of the CS membranes with different Al_2O_3 contents. From these figures, highly porous structure was found in sample A [Figure 2(a)], which may enhance the liquid electrolyte holding capacity. On the other hand, few pores were observed in the sample B [Figure 2(b)] because a small amount of powders were buried in the PVDF binder, which resulted in the formation of a dense polymer phase inevitably increasing the difficulty in filling with electrolyte. Moreover, sample A displayed uniform pore distribution. Uniform distribution and a tortuous structure of the pores are both highly desirable since the former ensures a uniform current distribution throughout the separator and the latter suppresses the growth of dendritic lithium.[7] It could be also seen from the cross section SEM of sample A [Figure 2(c)] that nano-sized Al_2O_3 particles were dispersed in the PVDF matrix, and these structures had not only good thermal stability due to the existence of the inorganic materials, but also high ionic conductivity that originated from the large uptake of the liquid electrolytes caused by the liquid-phylic tendency of ceramic particles[13] and more channels for the reaction of Li^+ insertion/extraction. Therefore, sample A with a fixed P/B ratio of 1.5 was worth further research.

To evaluate the pore size in the sample A with high Al_2O_3 content, the pore size distribution (Figure 3) of the sample A was measured. The mercury porosimetry analysis technique is based on the intrusion of mercury into a porous structure under stringently controlled pressures. Using a mercury intrusion porosimeter, the pore size distribution of the sample was expressed using the logarithmic differential intrusion volume as a function of pore diameter. Sample A was subjected to a pressure cycle starting at approximately 20 psia, increasing to 60000 psia in predefined steps to give pore size information. It could be found in Figure 3 that the pore size distribution of the sample A had a peak between 3 and 10 nm, and average pore diameter was 12.4 nm which was smaller than powder particle size, ca. 30 nm. Therefore, the sample A displayed small pore size and narrow pore size distribution. This indicates that ball milling plays an important role in yielding homogeneous membranes

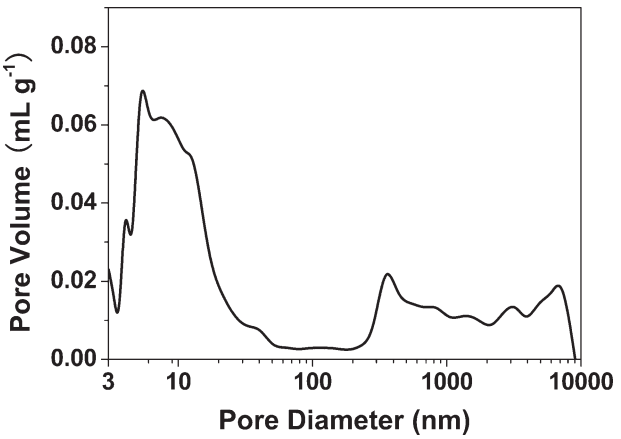

Figure 3. Pore size distribution in the sample A with high Al_2O_3 content.

with small pore size and sample A is expected to obtain superior electrochemical performance.

Figure 4 shows the FTIR-ATR spectra of Al_2O_3 powder, sample A and PVDF membrane. As expected, sample A revealed the main typical spectra of PVDF, i.e. the absorption peaks appearing at 1400 and 1168 cm^{-1} were assigned to the vibration of PVDF, and the absorption peak appearing at 1070 cm^{-1} was assigned to the C—F bond stretching vibration modes of PVDF along with amorphous phases at 880 and 840 cm^{-1}. This indicates that the reaction in the complex would not damage the chemistry structure of PVDF.[32] In addition, for PVDF membrane, all peaks were found to be intense and intensive absorption bands at 612, 764, 797, and 976 cm^{-1} corresponded to large amount of α crystal phase, which complied well with those described in literature.[33,34] However, these four significant peaks had vanished and the peak located at 633 cm^{-1} corresponding to Al_2O_3[35] was clearly observed in sample A, revealing that the addition of Al_2O_3 particles could influence the crystalline phase of semi-crystalline PVDF to some extent.[32]

In order to further examine the feasibility of using Al_2O_3-PVDF composite membranes as separators in the cell system based on $Li_4Ti_5O_{12}$-TiO_2 anode, the electrochemical performance of the coin-type half-cell using sample A was evaluated through galvanostatic discharge/charge experiments. Figure 5 shows the charge and discharge curves of lithium-ion cells assembled with sample A at a current density of 0.1 A g^{-1}. As seen in Figure 5, both the discharge and charge curves had two stable voltage

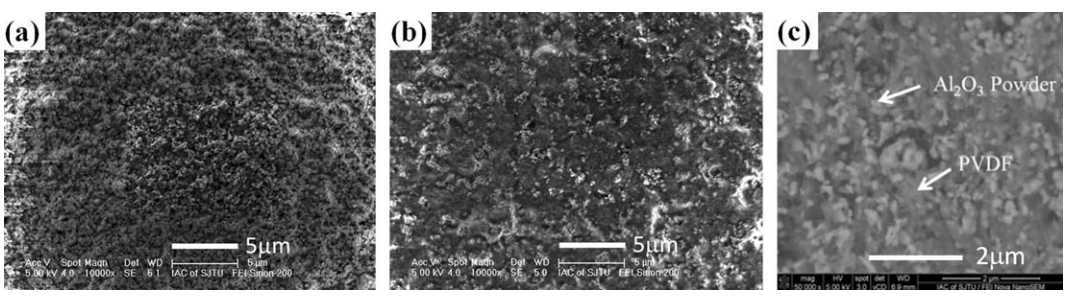

Figure 2. SEM photographs of the surface of the sample A (a), sample B (b), and (c) cross-section of sample A.

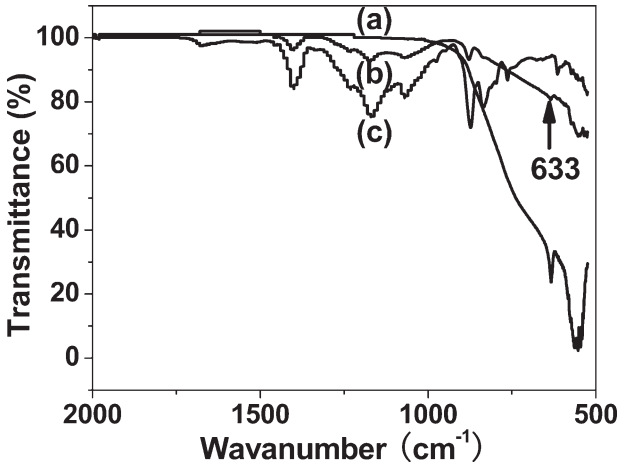

Figure 4. The FTIR-ATR spectra of Al_2O_3 powder (a), sample A (b), and (c) PVDF membrane.

plateaus due to the formation of the two phases of $Li_4Ti_5O_{12}$ and TiO_2,[36] and the fifth specific discharge capacity of the sample A was approximately 135 mAh g^{-1}.

Figure 6 shows the discharge capacity versus cycle number for the test cells using sample A subjected to 10 cycles at room temperature. It may be seen that the cell using sample A had an excellent cycle life, clearly demonstrating a low degree of capacity loss over a long number of cycles. After the 10th cycle, the discharge capacity of the cell using sample A was measured to be 131 mAh g^{-1} under a constant current density of 0.1 A g^{-1}. This is due to the fact that Li^+ insertion/extraction is sufficient at this relatively low current rate.[37] Moreover, since the average pore size of the sample A with the help of ball milling was reduced and its distribution became narrow, the ability to keep electrolytes in the pores might be higher because of the difference of capillary action. This capillary action that helps avoiding a lack of electrolytes, and high surface area of the dispersed nano-sized Al_2O_3 fillers, can improve cycling stability of the cells. The result confirms the excellent efficiency of the Al_2O_3-PVDF composite separators to conduct lithium ions

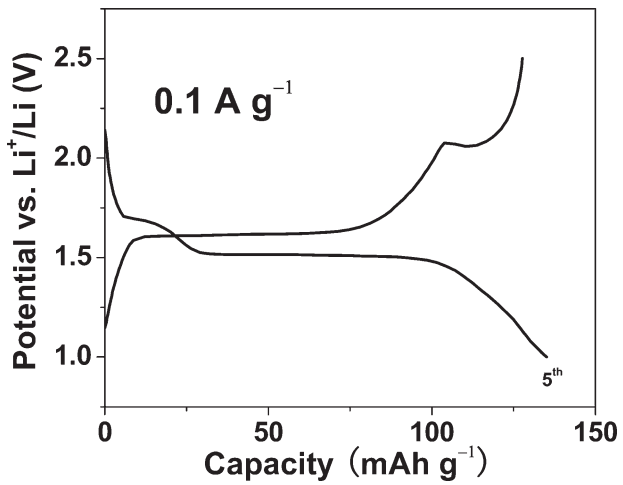

Figure 5. Charge and discharge curves of the cells assembled with sample A under a constant current density of 0.1 A g^{-1}.

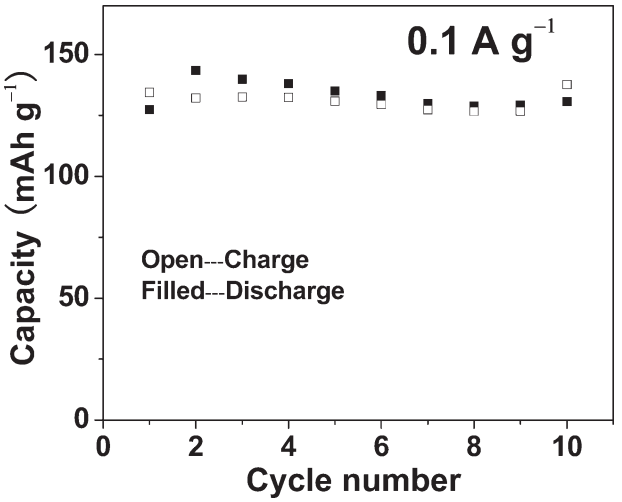

Figure 6. Cycle performance of the cells assembled with sample A under a constant current density of 0.1 A g^{-1}.

between electrodes during cycling process. Therefore, the Al_2O_3-PVDF composite separators prepared from ball-milling-assisted tape casting can be successfully applied in cell systems using $Li_4Ti_5O_{12}$-TiO_2 as the selected anode and $LiClO_4$-EC/DEC solutions as electrolyte.

CONCLUSIONS

This study reports on the preparation and characterization of Al_2O_3-added composite separators obtained by dispersing and ball milling of Al_2O_3 particles in PVDF polymer for lithium-ion batteries. The inorganic-based composite separator with high Al_2O_3 content possessed good thermal stability and highly porous structure, and ball milling was beneficial in yielding homogeneous separators with small pore size, which can trap more liquid electrolytes. The composite cell that comprised a $Li_4Ti_5O_{12}$-TiO_2, a lithium foil as counter electrode and a composite separator with high Al_2O_3 content was assembled and evaluated. After the 10th cycle, the cell achieved the discharge capacities of as much as 131 mAh g^{-1}, and showed high cycling stability. These results suggest that the Al_2O_3-PVDF composite separator prepared from ball-milling-assisted tape casting is a promising separator for the cell systems using $Li_4Ti_5O_{12}$-TiO_2 as the selected anode and $LiClO_4$-EC/DEC solutions as electrolyte, which contributes to expand the interest for the applications in the other types of lithium ion batteries.

ACKNOWLEDGMENTS

This work was supported by the National High-Tech R&D Program (863 Program) (Grant No. 2009AA05Z113), and the National Natural Science Foundation of China (Grant No. 50672058).

AUTHOR CONTRIBUTIONS

Of all listed authors, Huifeng Wang is in charge of the materials synthesis and characterization, and Haibin Li and Lijun Yu contribute significantly to revising the article. Moreover, Yanmei Jiang and Kaixue Wang provide technical assistance with electrochemical measurement.

REFERENCES

1. Kim, M.; Park, J. H. *J. Power Sources* **2012**, *212*, 22.
2. Arora, P.; Zhang, Z. M. *Chem. Rev.* **2004**, *104*, 4419.
3. Raab, M.; Scudla, J.; Kozlov, A. G.; Lavrentyev, V. K.; Elyashevich, G. K. *J. Appl. Polym. Sci.* **2001**, *80*, 214.
4. Liu, X. J.; Kusawake, H.; Kuwajima, S. *J. Power Sources* **2001**, 97–98, 661.
5. Liang, Y. Z.; Ji, L. W.; Guo, B. K.; Lin, Z.; Yao, Y. F.; Li, Y.; Alcoutlabi, M.; Qiu, Y. P.; Zhang, X. W. *J. Power Sources* **2011**, *196*, 436.
6. Cho, T. H.; Tanaka, M.; Onishi, H.; Kondo, Y.; Nakamura, T.; Yamazaki, H.; Tanase, S.; Sakai, T. *J. Power Sources* **2008**, *181*, 155.
7. Zhang, S. S. *J. Power Sources* **2007**, *164*, 351.
8. Augustin, S.; Hennige, V.; Horpel, G.; Hying, C. *Desalination* **2002**, *146*, 23.
9. Fu, D.; Luan, B.; Argue, S.; Bureau, M. N.; Davidson, I. J. *J. Power Sources* **2012**, *206*, 325.
10. Lee, Y. M.; Kim, J. W.; Choi, N. S.; Lee, J. A.; Seol, W. H.; Park, J. K. *J. Power Sources* **2005**, *139*, 235.
11. Croce, F.; Appetecchi, G. B.; Persi, L.; Scrosati, B. *Nature* **1998**, *394*, 456.
12. Persi, L.; Croce, F.; Scrosati, B.; Plichta, E.; Hendrickson, M. A. *J. Electrochem. Soc.* **2002**, *149*, A212.
13. Appetecchi, G. B.; Romagnoli, P.; Scrosati, B. *Electrochem. Commun.* **2001**, *3*, 281.
14. Croce, F.; Scrosati, B. *Adv. Membr. Technol.* **2003**, *984*, 194.
15. Kim, M.; Han, G. Y.; Yoon, K. J.; Park, J. H. *J. Power Sources* **2010**, *195*, 8302.
16. Jeong, H. S.; Noh, J. H.; Hwang, C. G.; Kim, S. H.; Lee, S. Y. *Macromol. Chem. Phys.* **2010**, *211*, 420.
17. Jeong, H. S.; Hong, S. C.; Lee, S. Y. *J. Membr. Sci.* **2010**, *364*, 177.
18. Park, J. H.; Cho, J. H.; Park, W.; Ryoo, D.; Yoon, S. J.; Kim, J. H.; Jeong, Y. U.; Lee, S. Y. *J. Power Sources* **2010**, *195*, 8306.
19. Zhang, S. S.; Xu, K.; Jow, T. R. *J. Power Sources* **2005**, *140*, 361.
20. Prosini, P. P.; Villano, P.; Carewska, M. *Electrochim. Acta* **2002**, *48*, 227.
21. Ding, Y. H.; Zhang, P.; Long, Z. L.; Jiang, Y.; Xu, F.; Di, W. *Sci. Technol. Adv. Mater.* **2008**, *9*. 015005.
22. Kim, K. M.; Park, N. G.; Ryu, K. S.; Chang, S. H. *Electrochim. Acta* **2006**, *51*, 5636.
23. Wachtler, M.; Ostrovskii, D.; Jacobsson, P.; Scrosati, B. *Electrochim. Acta* **2004**, *50*, 357.
24. Yang, C. C.; Chen, Y. C.; Lian, Z. Y.; Liou, T. H.; Shih, J. Y. *J. Solid State Electrochem.* **2012**, 16, 1815.
25. Stephan, A. M.; Nahm, K. S.; Kulandainathan, M. A.; Ravi, G.; Wilson, *J. Eur. Polym. J.* **2006**, *42*, 1728.
26. Jeong, H. S.; Lee, S. Y. *J. Power Sources* **2011**, *196*, 6716.
27. Subramania, A.; Sundaram, N. T. K.; Priya, A. R. S.; Kumar, G. V. *J. Membr. Sci.* **2007**, *294*, 8.
28. Zhang, Y. Q.; Zhang, G. D.; Du, T. D.; Zhang, L. Z. *Electrochim. Acta* **2010**, *55*, 5793.
29. Choi, J. A.; Kim, S. H.; Kim, D. W. *J. Power Sources* **2010**, *195*, 6192.
30. Mandal, S.; Rao, V.; Ray, A. K. *J. Mater. Sci.* **2004**, *39*, 5587.
31. Jeong, H. S.; Kim, D. W.; Jeong, Y. U.; Lee, S. Y. *J. Power Sources* **2010**, *195*, 6116.
32. Liu, F.; Abed, M. R. M.; Li, K. *J. Membr. Sci.* **2011**, *366*, 97.
33. Gregorio, R. *J. Appl. Polym. Sci.* **2006**, *100*, 3272.
34. Ostasevicius, V.; Milasauskaite, I.; Dauksevicius, R.; Baltrusaitis, V.; Grigaliunas, V.; Prosycevas, I. *Mechanika* **2010**, *6*, 78.
35. Zhu, Z. F.; Sun, H. J.; Liu, H.; Yang, D. *J. Mater. Sci.* **2010**, *45*, 46.
36. Rahman, M. M.; Wang, J. Z.; Hassan, M. F.; Wexler, D.; Liu, H. K. *Adv. Energy Mater.* **2011**, *1*, 212.
37. Rahman, M. M.; Wang, J. Z.; Hassan, M. F.; Chou, S. L.; Wexler, D.; Liu, H. K. J. *Power Sources* **2010**, *195*, 4297.